Verification of the Hexagonal Ray Tracing Module and the CMFD Acceleration in nTRACER

Seongchan Kim, Changhyun Lim, Young Suk Ban and Han Gyu Joo*
Seoul National University, 1 Gwanak-ro Gwankak-gu, Seoul, 08826, Korea
**Corresponding author: joohan@snu.ac.kr*

1. Introduction

nTRACER [1] is a direct whole core transport calculation code for 3D core analysis, which employs a planar Method Of Characteristics (MOC) calculation and Simplified P_3 (SP_3) axial calculation accelerated by 3D Coarse Mesh Finite Difference (CMFD) method. So far, modular ray and CMFD formulation of nTRACER are applicable in rectangular geometries, since the code was designed for general PWR cores analysis. However, fast reactor cores are mostly based on the hexagonal geometry to achieve high power density and in order to simulate these fast reactors, nTRACER needs to equip a calculation capability to deal with hexagonal geometries. The objective of the work is to implement and verify the hexagonal ray tracing module and the CMFD acceleration in nTRACER.

2. Implementation Strategy

nTRACER follows general hexagonal modular ray scheme, but it can also handle unstructured coarse mesh configuration which appears in hexagonal cores, such as non-hexagonal boundary pin cells and gap cells. In this section, the details of the modeling of hexagonal geometries and the unstructured CMFD formulation are introduced.

2.1 Modeling of Residual Regions

Residual regions between pin cells and assembly boundaries can be modeled in two different ways, *chopped model* and *elongated model*. In *chopped model*, all pin cells have the same hexagonal geometry as the left figure of Fig. 1, and the residual regions are chopped into pentagons. In *elongated model*, boundary pin cells are elongated into pentagons, and residual regions are defined as trapezoidal gap cells as the right figure of Fig. 1.

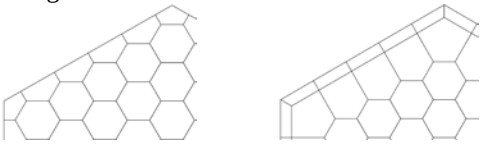

Fig. 1. *Chopped Model* and *Elongated Model* for the modeling of residual regions between pin cells and assembly boundaries.

DeCART, which is also direct whole core transport code, adopts *chopped model* [2]. On the other hand, nTRACER adopts *elongated model*. It is because, unlike *chopped model*, *elongated model* has a merit in explicit modeling of the assembly duct which wraps the assembly boundary in a band shape. Furthermore, with *elongated model*, the modeling applicability of nTRACER is extended so that it can simulate the core problem with multiple layers of ducts and the assemblies with various different pin pitches which appears in the hexagonal cores such like the ABR core.

2.2 General Formulation of Hexagonal CMFD

General formulation of hexagonal CMFD is required for the treatment of unstructured geometries which appear in hexagonal cores since the side lengths and the center to side distances are not identical through the core. Detailed formulations of unstructured CMFD are as follows.

The net current, $\tilde{D}_m$ and $\hat{D}_m$ defined at the surface between the m-th mesh and the m+1-th mesh can be written as Eq. (1), (2), and (3).

$$J_m = -\tilde{D}_m\left(\phi_{m+1}-\phi_i\right)-\hat{D}_m\left(\phi_{m+1}+\phi_i\right) \tag{1}$$

$$\tilde{D}_m = \frac{D_m D_{m+1}}{D_m l_{m+1}+D_{m+1} l_m} \tag{2}$$

$$\hat{D}_m = -\frac{-\hat{J}_m-\tilde{D}_m\left(\phi_{m+1}-\phi_m\right)}{\phi_{m+1}+\phi_m} \tag{3}$$

The final finite difference formulation [3] can be written as Eq. (4).

$$\sum_i\left(\tilde{D}_m^i-\hat{D}_m^i\right)S_{m+i}\phi_m-\sum_i\left(\tilde{D}_m^i+\hat{D}_m^i\right)S_{m+i}\phi_{m+i} +\Sigma_{t,m}\phi_m V_m = Q_m V_m \tag{4}$$

The center to side is defined as the vertical distance between the center of mass and the boundary as shown in Fig. 2.

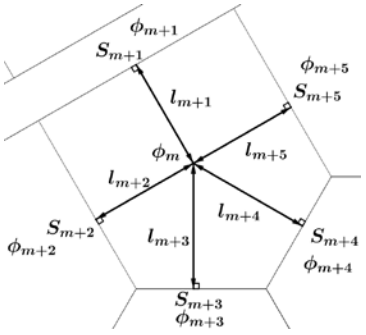

Fig. 2. Example of unstructured coarse mesh configuration

3. Performance Verification

To verify the implementation of the hexagonal ray tracing module and its CMFD acceleration, nTRACER performed several test core calculations. First, 2D C5G7 hexagonal variation benchmark [2] was performed for the verification of its elementary features. Then, 2D ABR C5G7 variation benchmark was performed to show its capability to handle a complex hexagonal core. And then, 3D C5G7 hexagonal variation benchmark with three different control rod insertions [2] were performed for the verification of the capability to handle 3D problems. nTRACER calculations were performed with 0.05 cm ray spacing, 4 azimuthal angles in $\pi/3$, and 2 polar angles in $\pi/2$ while utilizing 1/6 symmetry.

3.1. Effectiveness of CMFD Acceleration

Fig. 3 shows the error reduction behavior between sole MOC calculation and CMFD accelerated MOC calculation for 2D C5G7 hexagonal variation benchmark. The convergence criteria of k-eff, fission source and residual error were set to be less than 10^{-6}.

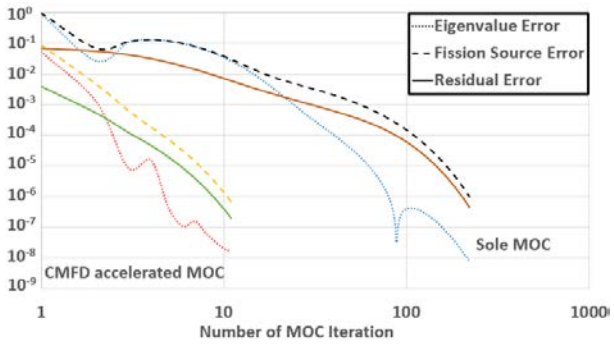

Fig. 3. Comparison of error reduction by CMFD acceleration for 2D C5G7 hexagonal variation benchmark

Hexagonal CMFD kernel reduced the number of MOC iteration as a factor of 20 and the computation time as a factor of 10 compared to the sole MOC calculation for 2D C5G7 hexagonal variation benchmark with 521 CMFD outer iterations. For 2D ABR C5G7 variation benchmark, hexagonal CMFD kernel reduced the number of MOC iteration as a factor of 82 and the computation time as a factor of 22 with 200 CMFD outer iterations.

Table 1. Reduction of number of MOC iteration and computation time by CMFD acceleration

Benchmark	Case	# of MOC Iteration	Computation Time (s)
2D C5G7 Hexagonal Variation	Sole MOC	222	276
	CMFD Accelerated	11	27
2D ABR C5G7 Variation	Sole MOC	735	9437
	CMFD Accelerated	9	437

3.2. 2D C5G7 Hexagonal Variation Benchmark

The nTRACER solutions for 2D C5G7 hexagonal variation benchmark [2] are compared to the multi-group Monte Carlo solution performed by McCARD [4] which used 2,000,000 particles per cycle, 500 inactive cycles, and 1000 active cycles. The results are summarized in Table 2.

Table 2. Reactivity and absolute pin power error of nTRACER in 2D C5G7 hexagonal variation benchmark

k-eff	McCARD (σ, pcm)	1.16243 (2)
	nTRACER ($\Delta\rho$, pcm)	1.16231 (-9)
Pin Power Error(1), %	Max	1.94
	RMS	0.50

(1) $\sigma < 0.27\%$

The pin power distribution error of nTRACER is shown in Fig. 4. At the outmost fuel assemblies, nTRACER has 1% higher pin power than that of McCARD, and lower pin power at the innermost fuel assemblies. The maximum pin power error is located at the corner of inner most assembly because of the relatively large size of the Flat Source Region (FSR) at the corner fuel pin in *elongated model*.

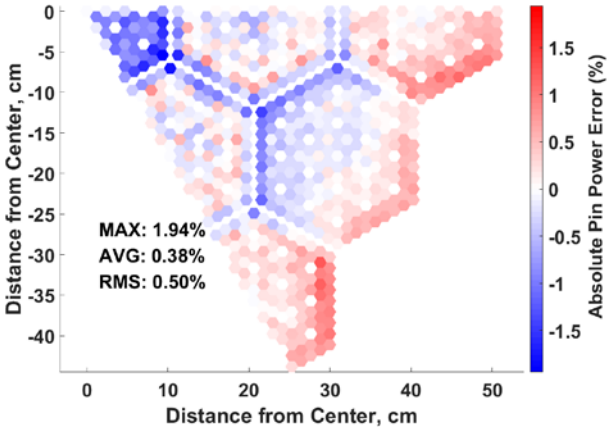

Fig. 4. Absolute pin power distribution error of nTRACER compared to McCARD for 2D C5G7 hexagonal variation benchmark

3.3. 2D ABR Variation Benchmark with C5G7 XS

The ABR (Advanced Burner Reactor) core was designed for the study of future fast reactor designs [5]. Thus, there are a lot kind of assembly configurations as shown in Fig. 5. The distinctive geometries of this benchmark are the different pin size through assembly types and the double-layered duct at the control assemblies.

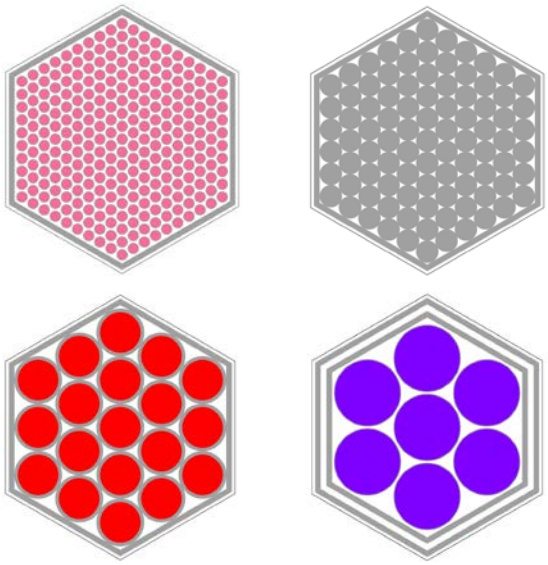

Fig. 5. Assembly configuration of ABR metallic benchmark (Left upper: Fuel assembly, Right upper: Reflector assembly, Left lower: Shield assembly, Right lower: Control assembly)

The original 3D ABR core is simplified into 2D core and the composition are replaced by that of C5G7 benchmark [6] as summarized in Table 3. nTRACER performed this modified ABR problem for the examination of its applicability in hexagonal core with a complex geometry.

Table 3. Material substitution in 2D ABR C5G7 variation benchmark

ABR metallic benchmark	ABR C5G7 variation benchmark
Fuel in inner core	UO_2-clad
Fuel in outer core	4.3% MOX
Na	Moderator
HT-9	Guide tube
Natural B_4C	Control rod

The results of nTRACER compared to McCARD reference are summarized in Table 4. Though the reactivity error and the maximum pin power error are slightly larger than 2D C5G7 variation benchmark case, it showed better agreement in the RMS pin power.

Table 4. Reactivity and absolute pin power error of nTRACER in 2D ABR C5G7 variation benchmark

k-eff	McCARD (σ, pcm)	1.19693 (3)
	nTRACER($\Delta\rho$, pcm)	1.19773 (56)
Pin Power Error(1), %	Max	2.50
	RMS	0.44

(1) $\sigma < 0.65\%$

The pin power error distribution is plotted in Fig. 6. nTRACER has higher pin power at outer core and lower pin power at inner core compared to McCARD. The reason of power error peak around the boundary of control assembly is due to the relatively large size of the FSR in the control assembly where the pin pitch is large.

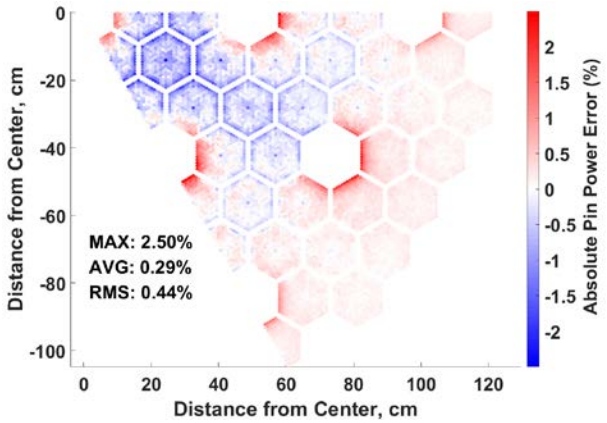

Fig. 6. Absolute pin power distribution error for 2D ABR C5G7 variation benchmark

3.4. 3D C5G7 Hexagonal Variation Benchmark

Three 3D problems with different rod positions [2] are performed for the verification of the capability of nTRACER to solve 3D hexagonal cores. In unrodded case, all control rods are pulled out up to the reflector plane as TA in Fig. 7. In rodded A case, control rods in UA-1 are inserted one third of active fuel length as TB. In rodded B case, control rods in UA-1 are inserted as TC and control rods in UA-2 are inserted as TB. nTRACER performed 3D problems with 3.57 cm of 12 axial meshes for fuel planes and 5.355 cm of 4 axial meshes for reflector planes

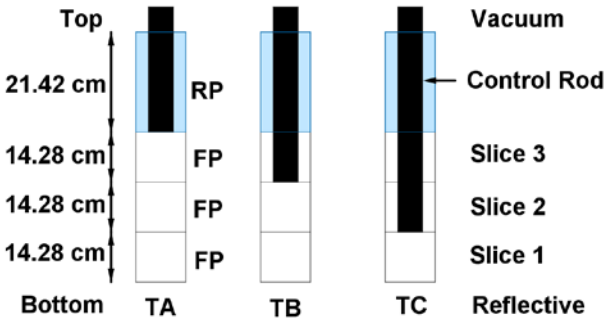

Fig. 7. Axial rod insertion types for 3D C5G7 hexagonal variation benchmark

Also for the 3D problem, nTRACER showed good agreement in both k-eff and pin power distribution compared to the McCARD as it is summarized in Table 5. The 3D pin power distribution was normalized to unity for each slice. McCARD performed 3D problems with axial meshes same as nTRACER for a one-to-one comparison of pin power between McCARD and nTRACER.

Table 5. Reactivity and absolute pin power error of nTRACER in 3D C5G7 hexagonal variation benchmark

		Unrodded	Rodded A	Rodded B
McCARD(1)	k-eff	1.12273	1.11886	1.10264
	σ	0.00001	0.00001	0.00001
k-eff of nTRACER ($\Delta\rho$, pcm)		1.12280 (6)	1.11890 (3)	1.10267 (2)
Slice 1 Pin Power Error, %	Max.	2.13	2.01	1.92
	RMS	0.49	0.48	0.55
Slice 2 Pin Power Error, %	Max.	2.08	2.17	2.35
	RMS	0.51	0.47	0.55
Slice 3 Pin Power Error, %	Max.	2.31	2.93	3.07
	RMS	0.56	0.58	0.64
2D Integrated Pin Power Error, %	Max.	2.02	1.86	2.02
	RMS	0.47	0.47	0.52

(1) Pin Power $\sigma < 0.50\%$

The absolute error in radially integrated axial pin power is plotted in Fig. 8. The relative axial position in Fig. 8 indicates the order of axial meshes. The maximum error of radially integrated pin power is 0.37% which appears at the last axial mesh.

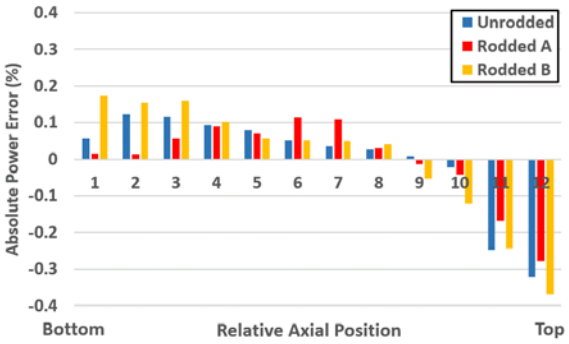

Fig. 8. Absolute error of nTRACER in radially integrated power distribution for 3D C5G7 hexagonal variation benchmark

4. Conclusion

The hexagonal ray tracing module and the CMFD acceleration have been successfully implemented in nTRACER. Unstructured hexagonal CMFD formulation is implemented in nTRACER based on the special representation of the hexagonal assembly, in which trapezoidal gap cells envelop boundary cells to handle the residual regions between pin cells and assembly boundaries. The hexagonal CMFD kernel effectively reduced the computation time as a factor of 10 for 2D C5G7 variation benchmark and 22 for 2D ABR C5G7 variation benchmark. Results of nTRACER for 2D C5G7 hexagonal variation benchmark and 2D ABR C5G7 variation benchmark agreed to McCARD within 56 pcm error in the reactivity and RMS 0.50% in the pin power distribution. Especially in 2D ABR C5G7 variation benchmark calculation, nTRACER proved its capability to solve the complex hexagonal core problem comprised of multiple layers of ducts and the assemblies with various different pin pitches. For 3D C5G7 hexagonal variation benchmark, nTRACER solution matched well with McCARD with the maximum 6 pcm error in the reactivity and the maximum RMS 0.52% error in the 2D integrated pin power distribution. The maximum absolute power error was 0.37% in radially integrated axial pin power. Since verifications in this work were based on the C5G7 benchmark cross-section, it is necessary to perform with 47 group condensed cross-section in nTRACER comparing with continuous McCARD solution.

ACKNOWLEDGEMENTS

This work was supported by the Nuclear Safety Research Program through the Korea Foundation Of Nuclear Safety (KoFONS), granted financial resource from the Nuclear Safety and Security Commission (NSSC), Republic of Korea. (No. 1602003)

REFERENCES

[1] Y. S. Jung, C. B. Shin, C. H Lim and H. G. Joo, Practical Numerical Reactor Employing Direct Whole Core Neutron Transport and Subchannel Thermal/Hydraulic Solvers, Annals of Nuclear Energy, 62, 357-374, 2013.
[2] J. Y. Cho, K. S. Kim, H. J. Shim, J. S. Song, C. C. Lee, and H. G. Joo, Whole Core Transport Calculation Employing Hexagonal Modular Ray Tracing and CMFD Formulation, Journal of nuclear science and technology, 45.8: 740-751, 2008.
[3] K. S. Kim, and M. D. Deheart, Unstructured Partial-and net-current Based Coarse Mesh Finite Difference Acceleration Applied to the Extended Step Characteristics Method in NEWT, Annals of Nuclear Energy, 38.2: 527-534, 2011.
[4] H. J. Shim, B. S. Han, J. S. Jung, H. J. Park, C. H. Kim, McCARD: Monte Carlo Code for Advanced Reactor Design and Analysis, Nucl. Eng. Technol., 44[2], 161, 2012.
[5] T. K. Kim, W. S. Yang, C. Grandy, and R.N. Hill, Core Design Studies for a 1000MW_{th} Advanced Burner Reactor, Annals of Nuclear Energy, 36.3: 331-336, 2009.
[6] E. E. Lewis, M. A. Smith, N. Tsoulfanidis, G. Palmiotti, T. A. Taiwo, R. N. Blomquist, Benchmark Specification for Deterministic 2-D/3-D MOX Fuel Assembly Transport Calculations without Spatial Homogenization (C5G7 MOX), NEA/NSC 280, 2001.
[7] W. Bernnat, Benchmark for Neutronic Analysis of Sodium-cooled Fast Reactor Cores with Various Fuel Types and Core Sizes, Report NEA/NSC, 2015.